Pergamon

J. Mech. Phys. Solids, Vol. 46, No. 9, pp. 1637–1653, 1998

Printed in Great Britain
0022–5096/98 $—see front matter

PII: S0022–5096(97)00042–2

ON KINK-BAND PROPAGATION IN FIBER COMPOSITES

B. BUDIANSKY,†* N. A. FLECK‡ and J. C. AMAZIGO§

†Division of Engineering and Applied Sciences, Harvard University, Cambridge, MA 02138, U.S.A., ‡Engineering Department, Cambridge University, Cambridge CB2 1PZ, U.K., §Department of Mathematics, University of Nigeria, Nsukka, Nigeria

(*Received* 24 *March* 1997; *in revised form* 13 *June* 1997)

ABSTRACT

Two kinds of kink-band propagation in the compression of aligned-fiber composites are studied analytically: band broadening, discovered experimentally by Moran, Liu and Shih in 1995, in which a uniform kink band grows in the direction of loading at constant stress under increasing deformation; and transverse kink propagation, in which a kink band traverses a specimen quasi-statically under constant overall shortening. The analysis is based on a 1-D, geometrically nonlinear couple-stress theory of composite kinking that takes elastic fiber bending resistance into account together with idealized nonlinear stress–strain relations, but assumes non-breaking fibers. Simple results for the band-broadening and transverse propagation stresses are deduced, and their significance is discussed. © 1998 Elsevier Science Ltd. All rights reserved.

Keywords: A. kinking, B. fiber-reinforced composite, B. polymeric materials.

INTRODUCTION

Elementary analyses of localized kinking under compression of aligned-fiber polymer-matrix composites (Budiansky and Fleck, 1993), considered together with experimental data, provide compelling evidence that compressive kinking strength is governed primarily by the yield strength in shear of the composite, and by fiber misalignment. The indeterminacy of misalignments accounts for the notorious scatter in kinking data. (For some general reviews of kinking studies, see Budiansky and Fleck, 1994; Schultheisz and Waas, 1996; Waas and Schultheisz, 1996; Fleck, 1997.) On the basis of various geometrical and physical models of the composite, detailed 2-D finite-element calculations have recently been used to study the initiation, metamorphosis, and propagation of kink-bands in the presence of various initial distributions of fiber misalignment or notches (e.g., Fleck and Shu, 1995; Kyriakides *et al.*, 1995; Sutcliffe and Fleck, 1996; Kyriakides and Ruff, 1997). Such numerical studies provide useful insights into the kinking process, and also serve to assess the accuracy and relevance of elementary analyses. We note that fiber fracture has not yet been incorporated into 2-D finite-element calculations; but fiber fracture can generally be expected to occur only after the peak compressive stress has been attained (Fleck *et al.*, 1995).

* To whom correspondence should be addressed. E-mail: budiansky@harvard.edu.

In this paper we use 1-D analyses to explore two kinds of steady-state kink propagation: band broadening, in which an established kink band grows in the direction of loading, and transverse propagation, in which a kink band travels across the width of a composite specimen. Remarkably, band broadening without fiber fracture was discovered experimentally only recently by Moran *et al.* (1995). On the other hand, transverse propagation (which precedes band broadening) is ubiquitous, though often dynamic, and not usually steady-state. Both types of propagation have been studied theoretically on the basis of various physical models (e.g. Fleck and Budiansky, 1991; Sutcliffe and Fleck, 1994; Moran *et al.*, 1995; Liu and Shih, 1996). Our aim here is to present some fairly rigorous studies of the mechanics of band broadening and transverse propagation, including the effects of fiber bending resistance. With the further use of idealized constitutive models, succinct results will be shown for both types of kink propagation. Because compressive kinking strength is a random variable sensitive to initial imperfections, we will discuss briefly the possibility (Moran *et al.*, 1995) of adopting one or another of the kink propagation stresses as a rational working stress for design purposes.

REVIEW OF BASIC KINKING THEORY

To set the stage, we will summarize briefly some basic results of the elementary theory of kinking (Budiansky and Fleck, 1993). We show in Fig. 1 the conventional picture of a kink band oriented at an angle β, within which the fibers, originally misaligned by $\bar{\phi}$ with respect to the direction of loading, have rotated by the additional angle ϕ under the compressive stress σ. For ϕ and $\bar{\phi}$ small, equilibrium requires that

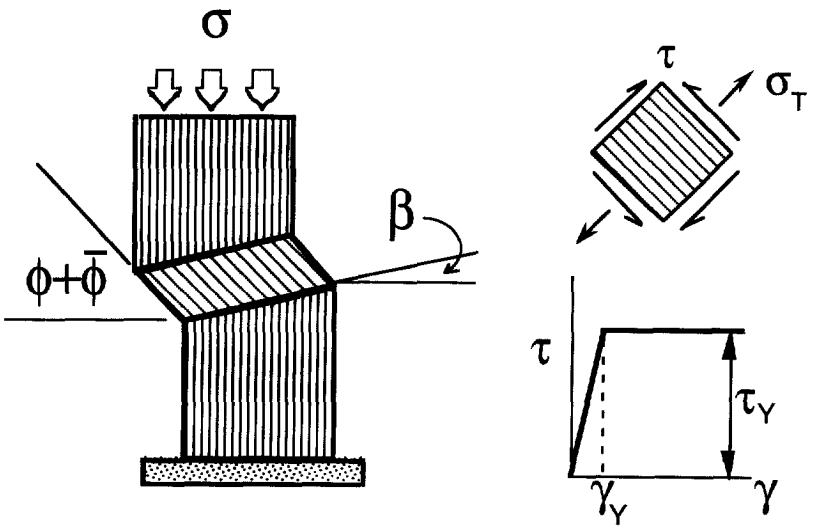

Fig. 1. Kink band, stresses in band, shear stress vs shear strain.

the shear stress τ and the tensile transverse stress σ_T defined in Fig. 1 be related to the applied compressive stress σ by

$$\sigma = \frac{\tau + \sigma_T \tan\beta}{\bar{\phi} + \phi} \tag{1}$$

and, for inextensional fibers, the shear strain γ and the transverse strain ε_T are given by

$$\begin{cases} \gamma = \phi \\ \varepsilon_T = \phi \tan\beta \end{cases} \tag{2}$$

Dropping the contribution of σ_T to σ, and adopting the elastic–ideally-plastic relation between τ and γ sketched in Fig. 1, we find that σ maximizes at $\phi = \gamma_Y$; this gives the lower-bound estimate

$$\sigma_c = \frac{\tau_Y}{\bar{\phi} + \gamma_Y} \tag{3}$$

for the critical kinking stress. In the limiting case $\bar{\phi} = 0$, this gives the Rosen (1965) result $\sigma_c = G$, where G is the elastic shear modulus of the composite; for $\gamma_Y = 0$, we get the Argon (1972) estimate $\sigma_c = \tau_Y/\bar{\phi}$.

Two points deserve emphasis. Even though eqn (3) does not contain β, comparisons made by Budiansky and Fleck (1993) indicate that over a reasonable range (say, up to $\beta = 40^\circ$) it provides a fair approximation to critical stresses derived for strain-hardening composites, with interactive effects of τ and σ_T taken into account, and τ_Y equal to a nominal yield stress. Second, the compressed composite is very imperfection-sensitive. For example, with $\bar{\phi} \approx 1.7^\circ$ and $\gamma_Y \approx 0.01$, eqn (3) gives $\sigma_c/G \approx 1/4$ and $\sigma_c/\gamma_Y \approx 25$; small changes in $\bar{\phi}$ overwhelm the effects of σ_T and β.

Another fact to be noted is that fiber fracture does not influence σ_c. The detailed studies of Fleck *et al.* (1995), in which fiber bending resistance is considered, show that fiber fracture occurs while the compressive load is dropping, at rotations much larger than those corresponding to the attainment of maximum load. This holds even if the fibers have no tensile strength; for this case, a simple approximate formula for the fiber rotation at fiber fracture, that follows from the analyses by Budiansky (1983) and Fleck *et al.* (1995), gives

$$\phi_{\text{fracture}} \approx \left(\frac{2\tau_Y}{E}\right)^{1/3} \tag{4}$$

where E is the Young's modulus of the composite. For the plausible value $\tau_Y/E = 0.0004$, this gives $\phi_{\text{fracture}} = 0.09$—much larger than the value $\phi = \gamma_Y$ at which σ_c is reached.

BAND BROADENING: OBSERVATIONS

In recent tests, Moran *et al.* (1995) and Moran and Shih (1998) observed the longitudinal kink-band broadening shown schematically in Fig. 2. The composite was

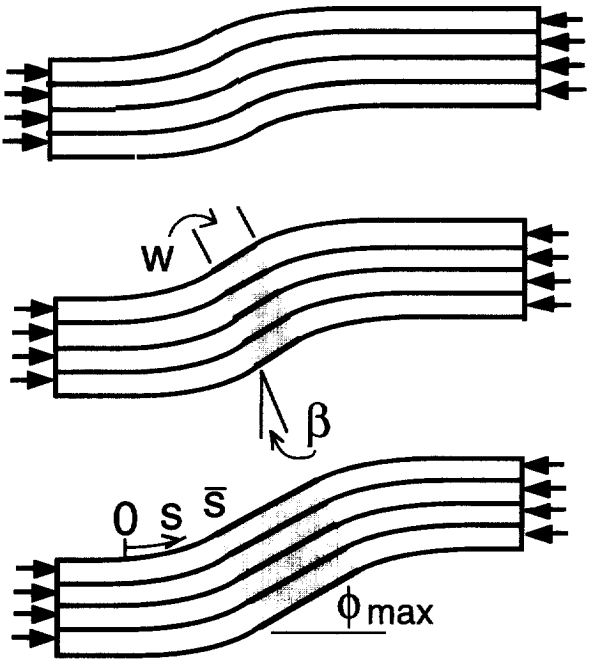

Fig. 2. Band broadening without fiber fracture.

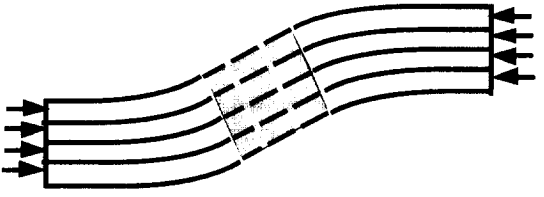

Fig. 3. Band broadening with multiple fiber fragments.

composed of 60% IM7 fibers in a PEEK matrix and the broadening evidently occurred without fiber fracture and at constant applied stress. The growing band of straight fibers, shown shaded, remained inclined at an angle ϕ approximately equal to twice the band orientation $\beta \approx 20^\circ$. This kind of fracture-free broadening was later seen by Fleck *et al.* (1997) in an IM8/PEEK composite.

Band broadening of the type illustrated in Fig. 3, in which the straight portion of the broadening band consists of broken segments of approximately equal length, has recently been observed by Sivashanker *et al.* (1996), Kyriakides and Ruff (1997), and Vogler and Kyriakides (1997). In these cases the composite contained AS4 carbon fibers, less strong and less stiff than IM7 and IM8. We will study only fracture-free band broadening in this paper, but we will also determine the magnitudes of fiber strength that permit its occurrence.

In the experiments of Vogler and Kyriakides (1997) the fiber rotation during broadening was found to exceed 2β somewhat. We will nevertheless use $\phi_{max} = 2\beta$ as a reasonable approximation, based on the idea of "lock-up", to be discussed.

LARGE-ROTATION, 1-D BENDING THEORY

We will develop here equations governing the response to compression of an aligned-fiber composite, appropriate for the study of band-broadening, and later, transverse kink propagation. The theory embodies couple stresses that account for the bending resistance of the fibers, but extends the linear analyses by Budiansky (1983) and Fleck *et al.* (1995) to large rotations. Small initial misalignments will be neglected in comparison with the much larger rotations that occur during the development of the broadening configuration.

We contemplate a geometry in which the kinking orientation is pre-set at β and (see Fig. 4) the fiber rotation ϕ is invariant along β-lines $x + y\tan\beta = \text{constant}$. Assuming inextensional fiber deformations, we can introduce the 1-D function $\phi(s)$, where s is distance along an arbitrary fiber, and define the longitudinal stress σ_L, transverse stress σ_T, sliding shear stress τ_S, transverse shear stress τ_T, and couple stress m, as shown in Fig. 4. These are all smeared-out true stresses, and are considered to be functions of s; σ_L and τ_S are parallel to the fibers, σ_T and τ_T act normal to the fibers, and m is the couple stress on the deformed plane normal to the fibers.

Distances along β lines do not change, but the rotated portions of the composite undergo transverse stretching. Let h denote the original thickness in the y-direction of a portion of the composite, and let $\bar{h}$ be the stretched thickness normal to the fibers (Fig. 4(d)). Then the transverse stretch ratio is

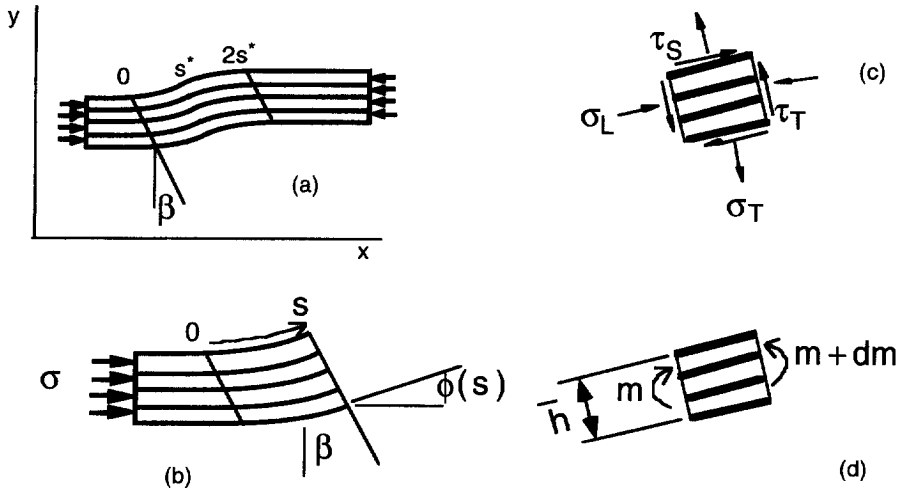

Fig. 4. Kinked composite, rotation $\phi(s)$, stresses, couple-stresses.

$$\frac{\bar{h}}{h} \equiv g(\beta, \phi) = \frac{\cos(\beta - \phi)}{\cos \beta} \tag{5}$$

The function $g(\beta, \phi)$ will appear frequently in the derivations that follow.

The assumptions of inextensionality and plane strain, i.e. zero strain in the thickness direction normal to the x–y plane, imply that the composite suffers a volumetric increase, also given by the ratio $g(\beta, \phi)$. (It is generally believed that this dilatation is accommodated by microcracking in the polymeric matrix.)

Force equilibrium in the direction normal to the fibres at the right end of the free body in Fig. 4(b) implies that

$$\sigma \cos \beta \sin \phi = \tau_T \cos(\beta - \phi) + \sigma_T \sin(\beta - \phi) \tag{6a}$$

and equilibrium in the fiber direction gives

$$-\sigma \cos \beta \cos \phi = \tau_S \sin(\beta - \phi) + \sigma_L \cos(\beta - \phi). \tag{6b}$$

These agree with the equilibrium equations given by Budiansky and Fleck (1993) for a constant-rotation kink, in which there is no bending and $\tau_S = \tau_T$. But now moment equilibrium of the element in Fig. 4(c, d) requires that

$$\frac{d}{ds}(mg) = (\tau_S - \tau_T)g \tag{7}$$

and this permits the elimination of τ_T from (6a) to give

$$\sigma \cos \beta \sin \phi + \cos \beta \frac{d}{ds}(mg) = \tau_S \cos(\beta - \phi) + \sigma_T \sin(\beta - \phi). \tag{8}$$

We will soon drop σ_T, but we keep it temporarily, in order to define strains via the principle of virtual work. For convenience (this is not crucial) say that ϕ vanishes at each end of the composite specimen in Fig. 4(a), and note that the shortening Δ is

$$\Delta = \int (1 - \cos \phi)\, ds \tag{9}$$

where the integration is over the original specimen length. We assert that strain variations $\delta\gamma$ and $\delta\varepsilon_T$, and bending-strain variations $\delta\kappa$, conjugate in the work sense to τ_S, δ_T, and m, satisfy the principle of virtual work

$$\sigma\delta \int (1 - \cos \phi)\, ds = \int (\tau_S \delta\gamma + \sigma_T \delta\varepsilon_T + m\delta\kappa) g(\beta, \phi)\, ds \tag{10}$$

for strain variations compatible with $\delta\phi(s)$ and all combinations of stresses (τ_S, σ_T) and couple stresses m that satisfy equilibrium. Eliminating σ via eqn (8), and doing one integration by parts, leads to

$$\int \left\{ \tau_S[\delta\gamma - \delta\phi] + \sigma_T[\delta\varepsilon_T - \delta\phi \tan(\beta - \phi)] + m\left[\delta\kappa - \delta\frac{d\phi}{ds}\right] \right\} g(\beta, \phi)\, ds = 0. \tag{11}$$

This implies the energetically consistent strain-rate definitions

$$\begin{cases} \dot{\gamma} = \dot{\phi} \\ \dot{\varepsilon}_T = \dot{\phi}\tan(\beta - \phi) \\ \dot{\kappa} = \mathrm{d}\dot{\phi}/\mathrm{d}s \end{cases} \tag{12}$$

which integrate to the strains

$$\begin{cases} \gamma = \phi \\ \varepsilon_T = \log\dfrac{\cos(\beta-\phi)}{\cos\beta} \equiv \log g(\beta, \phi) \\ \kappa = \mathrm{d}\phi/\mathrm{d}s \end{cases} \tag{13}$$

The first two of these agree with the results derived by Fleck and Budiansky (1991) for ϕ independent of s and $\bar{\phi} = 0$; the expression for ε_T is also consistent with the stretch ratio (5).

To complete the theoretical set-up we need constitutive relations. Transverse tension tests point to early failure at transverse strains less than 1% (e.g. Fleck and Jelf, 1995; Kyriakides *et al.*, 1995), and so at this point we will drop σ_T from the equilibrium eqn (8) as long as the transverse strain ε_T is positive. We then consider τ_S to be a function only of $\gamma = \phi$. (Here we abandon the unrealistic assumption made by Fleck and Budiansky (1991) that τ_S becomes zero when transverse failure occurs.) We note further that the transverse compressive strains that would want to occur for $\phi > 2\beta$ will be resisted elastically, at least initially, because matrix cracks will have closed, and so henceforth we make the simplifying "lock-up" assumption (Fleck and Budiansky, 1991), and say that ϕ cannot exceed 2β.

The bending will be presumed to be resisted elastically only by the fibers, with the bending moment M in each circular fiber given by

$$M = E_f \frac{\pi d^4}{64}\frac{\mathrm{d}\phi}{\mathrm{d}s} \tag{14}$$

where E_f is the fiber modulus and d its diameter. In terms of the fiber volume concentration c_f of the undeformed composite, the couple stress m in the deformed material is

$$m = \frac{c_f M}{g(\beta, \phi)(\pi d^2/4)} \tag{15}$$

and so, with the approximation $E \approx c_f E_f$ for the initial composite modulus, we get the bending constitutive relation

$$m = \frac{Ed^2}{16g(\beta, \phi)}\frac{\mathrm{d}\phi}{\mathrm{d}s}. \tag{16}$$

Using (16) in (8), with σ_T dropped, gives

$$\frac{Ed^2}{16}\frac{d^2\phi}{\mathrm{d}s^2} + \sigma\sin\phi = \tau_S(\phi)g(\beta, \phi) \tag{17}$$

for $\phi < 2\beta$. We will now neglect elastic strains in the relation $\tau_S(\phi)$, and suppose that τ_S jumps to a finite value for $\phi = 0^+$. We can then expect rotations $\phi(s)$ confined to a finite domain $(0, 2s^*)$, symmetrical about $s = s^*$, and satisfying $\phi(0) = \phi'(0) = 0$; this would lead to the picture in Fig. 4(a), with ϕ identically zero for $s < 0$ and $s > 2s^*$, and continuity of displacement, rotation, and bending moment maintained.

A first integral of (17), valid in $(0, s^*)$ for $\phi < 2\beta$, gives

$$\frac{Ed^2}{32}\left(\frac{d\phi}{ds}\right)^2 + \sigma(1-\cos\phi) = \int_0^{\phi} \tau_S(\tilde{\phi}) g(\beta, \tilde{\phi})\, d\tilde{\phi} \tag{18}$$

and since $d\phi/ds$ vanishes at $s = s^*$, the connection between σ and $\phi_{max} = \phi(s^*)$ is

$$\sigma = \frac{\int_0^{\phi_{max}} \tau_S(\phi) g(\beta, \phi)\, d\phi}{1-\cos\phi_{max}}. \tag{19}$$

Note that σ is generally a monotonically decreasing function of ϕ_{max}, starting at $\sigma = \infty$, and so the kinking stress, which occurs at small $\phi = O(\gamma_Y)$, is not captured by the theory. But as long as $\beta \gg \gamma_Y$, this should not matter much in the analysis of either band broadening or transverse kink propagation, both of which involve large rotations, up to $\phi = 2\beta$.

BAND BROADENING: CALCULATIONS

Lock-up will first occur when ϕ_{max} reaches the value 2β. The corresponding value of the applied stress σ given by eqn (19) is

$$\sigma_b = \frac{\int_0^{2\beta} \tau_S(\phi)\cos(\beta-\phi)\, d\phi}{\sin\beta \sin 2\beta}. \tag{20}$$

This is the band broadening stress! With the loading held constant at $\sigma = \sigma_b$, the successive configurations shown in Fig. 2 can evolve, with bent shapes identical to those at the initiation of lock-up emerging from a straight, locked interval of increasing size. All requirements of equilibrium and continuity remain fully satisfied during this band broadening. (It also has to be verified that in the locked region, where $m = 0$, the transverse stress given by

$$\sigma_T = [-\sigma_b \sin 2\beta - \tau_S(2\beta)]\cot\beta \tag{21}$$

according to eqn (8), is negative. This will always be true for $\tau'(\gamma) \geqslant 0$ and $\tau''(\gamma) \leqslant 0$.)

Because the basic equations of the theory were formulated to be consistent with virtual work principles, the result for the band-broadening stress should emerge from a simple energy calculation. Let w represent the length along the fibers in the locked portion of the kink band (see Fig. 2). The shortening during an increment δw during broadening is $\delta\Delta = \delta w(1-\cos 2\beta)$, and the additional work done by the sliding shear

stresses is $\delta w \int_0^{2\beta} \tau_S(\phi) g(\beta, \phi)\, d\phi$ per unit thickness of the composite. The virtual work equality

$$\sigma_b \delta w(1-\cos 2\beta) = \delta w \int_0^{2\beta} \tau_S(\phi) g(\beta, \phi)\, d\phi \tag{22}$$

recovers eqn (20).

Finally, we will display a convenient explicit result for the band-broadening stress, corresponding to the rigid-ideally-plastic idealization $\tau_S(\gamma) \equiv \tau_L$. (Here we distinguish τ_L from the value τ_Y (Fig. 1) that appears in the estimate (3) for the kinking stress. The yield stress τ_Y corresponds to very small shear strains, whereas τ_L should be regarded as representative of the stresses associated with the large rotations that occur during the evolution of band-broadening, and may be substantially higher than τ_Y. See, for example, the composite shear stress–strain curves measured by Kyriakides *et al.* (1995).) With $\tau_S(\phi) \equiv \tau_L$, eqn (22) becomes

$$\sigma_b \delta w(1-\cos 2\beta) = \delta w(2\tau_L \tan \beta) \tag{23}$$

and we get

$$\sigma_b = \frac{2\tau_L}{\sin 2\beta} \tag{24}$$

for the band-broadening stress. The transverse stress (21) in the locked region reduces to

$$\sigma_T = -\tau_L \cot \beta. \tag{25}$$

FIBER FRACTURE CRITERION

In order to assess the validity of the assumption that fiber fracture does not occur, we will calculate the maximum fiber tensile strain during band broadening. As before, we take the datum for distance s along a fiber to be the left-hand end of its curved region, as shown in Fig. 2. Fiber rotation begins at $s = 0$ and the fibers have rotated through 2β to a locked-up state at $s = \bar{s}$. The fiber tensile strain due to bending and longitudinal stress is given by

$$\varepsilon = \frac{d}{2} \frac{d\phi(s)}{ds} + \frac{g(\beta, \phi)\sigma_L(s)}{E} \tag{26}$$

for s in $(0, \bar{s})$. (The factor g in the second term reflects the effect of transverse stretching on the local composite stiffness in the fiber direction.) We will use the rigid–ideally plastic relation $\tau_S(\phi) \equiv \tau_L$, and introduce the nondimensional coordinate

$$S \equiv \frac{4s}{d} \sqrt{\frac{\tau_L}{E}} \tag{27}$$

to rewrite ε as

$$\varepsilon = 2\sqrt{\frac{\tau_L}{E}}\phi' + \frac{g\sigma_L}{E} \tag{28}$$

where ϕ and σ_L are now functions of S, and the primes denotes differentiation with respect to S. Setting $\sigma = \sigma_b$ and $\tau_S(\phi) \equiv \tau_L$ in eqn (18) gives the connection

$$\phi' = \sqrt{2\cos\beta[g(\beta,\phi) - 1]} \tag{29}$$

between ϕ' and ϕ in the curved portion of the kink during band broadening, and eqn (6b) provides

$$\frac{g\sigma_L}{E} = -\frac{\tau_L}{E}\left[\frac{\cos\phi}{\sin\beta\cos\beta} + \frac{\sin(\beta-\phi)}{\cos\beta}\right] \tag{30}$$

For each τ_L/E, the maximum ε_t can now be found by maximizing (28) with respect to ϕ in $(0, 2\beta)$; the maximum occurs for $\phi > \beta$, giving the curves shown in Fig. (5). Actually, the peak strain occurs so close to the point where $\phi = \beta$ that these results are indistinguishable from those given by explicit formula

$$\varepsilon_t = 2\sqrt{\frac{2\tau_L}{E}\tan\frac{\beta}{2}} - \frac{\tau_L}{E}\csc\beta \tag{31}$$

obtained by substituting $\phi = \beta$ in eqns (28)–(30).

Fig. (5) indicates combinations of β and τ_L/E for which fracture-free broadening would be possible for a given fiber breaking strain. For example, for a nominal fracture strain ε_f of $1\frac{1}{2}\%$, fracture-free band broadening with $\beta = 30^\circ$ could occur only for τ_L/E less than the unreasonably low value 0.0001; but for $\varepsilon_f = 2\%$ and $\beta = 15^\circ$, we would only need $\tau_L/E < 0.00045$.

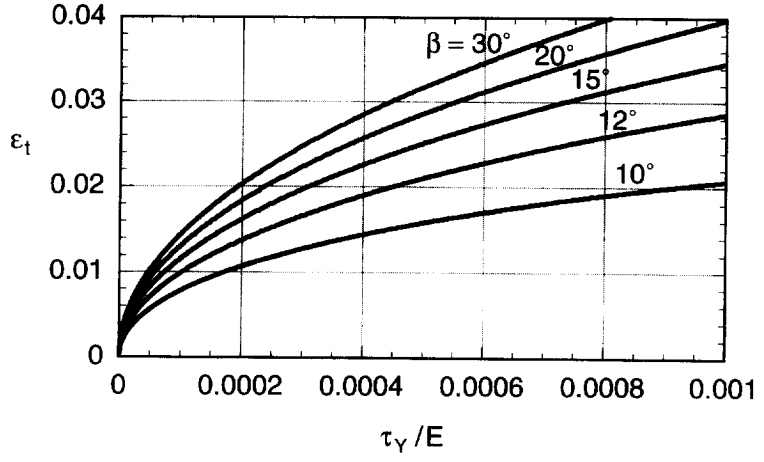

Fig. 5. Maximum fiber tensile strain during band broadening with unbroken fibers.

TRANSVERSE KINK PROPAGATION

We now contemplate a kink band propagating transversely at an angle β across a uniformly compressed specimen (Fig. 6(a)) into an unkinked region. Since the height L of the specimen is finite, the inclined kink would eventually have to run into the upper edge of the specimen. But we presume that the propagation will be essentially steady-state under constant end shortening Δ as long as the kink front remains far from the boundaries. Alternatively, the analysis that follows is also applicable (perhaps more so) to the horizontal steady-state propagation of a kink band inclined at β in the thickness direction (Fig. 6(b)).

We must now partially relinquish the assumption of fiber inextensionality, because the elastic shortening of the composite specimen due to fiber compression is likely to dominate the shortening Δ_{kink} associated with the fiber rotations, which occur over very small distances compared with the specimen length L. However, far back from the leading edge of the kink, the total shortening Δ may be approximated by

$$\Delta = \sigma_D L/E + \Delta_{kink} \tag{32}$$

where σ_D is the downstream boundary stress, E is the composite modulus, and Δ_{kink} is based on the inextensional, 1-D bending theory that we have developed. We anticipate that lock-up will occur downstream, and therefore, as indicated in Fig. 6, the downstream stress σ_D will be equal to the broadening stress σ_b. The downstream shortening Δ_{kink} will be written as the sum

$$\Delta_{kink} = \Delta_{bend} + w(1-\cos 2\beta) \tag{33}$$

where Δ_{bend} is the shortening due to fiber bending, and the last term is provided by the rotation of the locked portion of the kink. Then, for a kink propagating statically under a fixed shortening Δ, the upstream boundary stress σ_U must satisfy

$$\sigma_U L/E = \sigma_b L/E + \Delta_{bend} + w(1-\cos 2\beta) \tag{34}$$

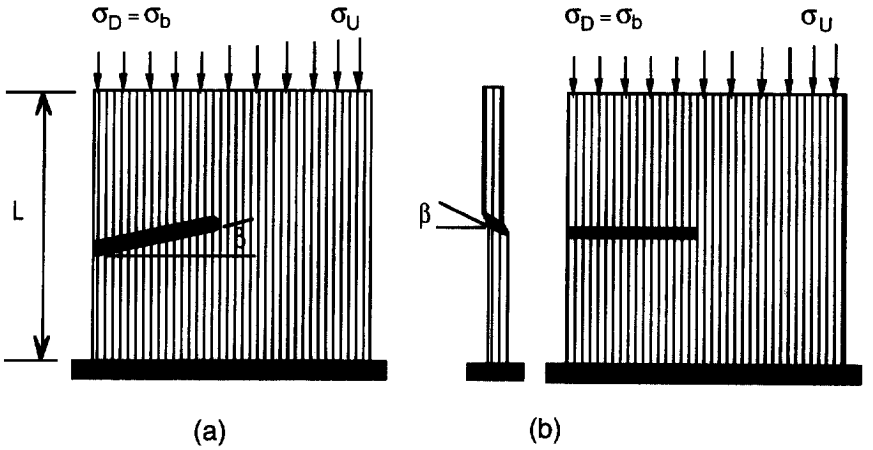

Fig. 6. Transverse kink propagation at kink-angle β: (a) in-plane; (b) through-the-thickness.

During steady kink propagation, upstream strain energy is converted to downstream strain and plastic shear dissipation. Accordingly, in units of energy per unit original width, per unit composite thickness

$$\frac{1}{2}\frac{\sigma_U^2 L}{E} = \frac{1}{2}\frac{\sigma_b^2 L}{E} + W_m + W_\tau + \sigma_b w(1-\cos 2\beta) \tag{35}$$

where W_m is the bending strain energy, W_τ is the work done by the sliding shear stresses in the bent portions of the kink, and the last term [see eqn (22)] is the work that has been done by the shear stress τ_L in the locked kink segment of length w. We can eliminate w from eqns (34)–(35) to get the result

$$\sigma_U = \sigma_b + \sqrt{\frac{2E}{L}(W_m + W_\tau - \sigma_b \Delta_{bend})} \tag{36}$$

For the upstream propagation stress.

To make this explicit, we adopt the rigid–plastic idealization $\tau_S(\phi) \equiv \tau_L$. The shortening due to bending is

$$\Delta_{bend} = 2\int_0^s (1-\cos\phi)\,ds = 2\int_0^{2\beta} \frac{1-\cos\phi}{d\phi/ds}\,d\phi \tag{37}$$

and making use of nondimensionalization (27) as well as the connection (29) between $d\phi/dS$ and ϕ leads to

$$\Delta_{bend} = d\sqrt{\frac{E}{\tau_L}}\sqrt{\frac{\tan\beta}{2}}\int_0^\beta \frac{1-g(\beta,\phi)\cos^2\beta}{\sqrt{g(\beta,\phi)-1}}\,d\phi. \tag{38}$$

Similarly [see eqn (16)] we have

$$W_m = 2\int_0^{\bar{s}} \frac{1}{2} mg\frac{d\phi}{ds}\,ds = \frac{Ed^2}{16}\int_0^{2\beta}\frac{d\phi}{ds}\,d\phi = \frac{\tau_L d}{2\sqrt{\tau_L/E}}\sqrt{2\cot\beta}\int_0^\beta \sqrt{g(\beta,\phi)-1}\,d\phi \tag{39}$$

and

$$W_\tau = 2\tau_L\int_0^{\bar{s}}\int_0^\phi g(\beta,\theta)\,d\theta\,ds = 2\tau_L\int_0^{2\beta}\frac{\tan\beta - \dfrac{\sin(\beta-\phi)}{\cos\beta}}{d\phi/ds}\,d\phi$$

$$= \frac{\tau_L d(2\tan\beta)^{3/2}}{4\sqrt{\tau_L/E}}\int_0^\beta \frac{d\phi}{\sqrt{g(\beta,\phi)-1}} \tag{40}$$

Putting (38)–(40) into eqn (36) yields the result

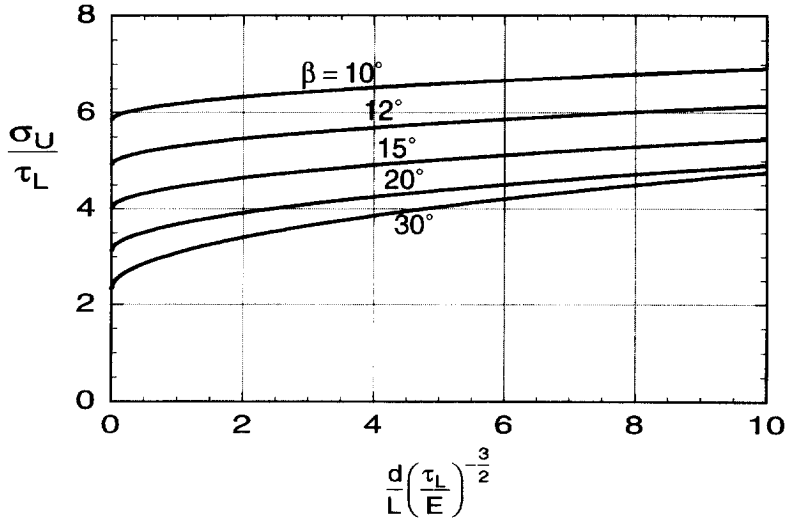

Fig. 7. Kink propagation stress for various kink angles β.

$$\frac{\sigma_U}{\tau_L} = \frac{\sigma_b}{\tau_L} + \left(\frac{d}{L}\right)^{1/2} \left(\frac{\tau_L}{E}\right)^{-3/4} \left(\frac{8}{\tan\beta}\right)^{1/4} \left\{\int_0^\beta \sqrt{g(\beta,\phi)-1}\, d\phi\right\}^{1/2} \tag{41}$$

for the propagation stress, illustrated in Fig. 7 for several values of β.

The size w of the locked part of the downstream kink may now easily be found from eqn (34). For the range of parameters in Fig. 7, w does indeed turn out positive, verifying the presumption of downstream lock-up. The results are shown non-dimensionally in Fig. 8.

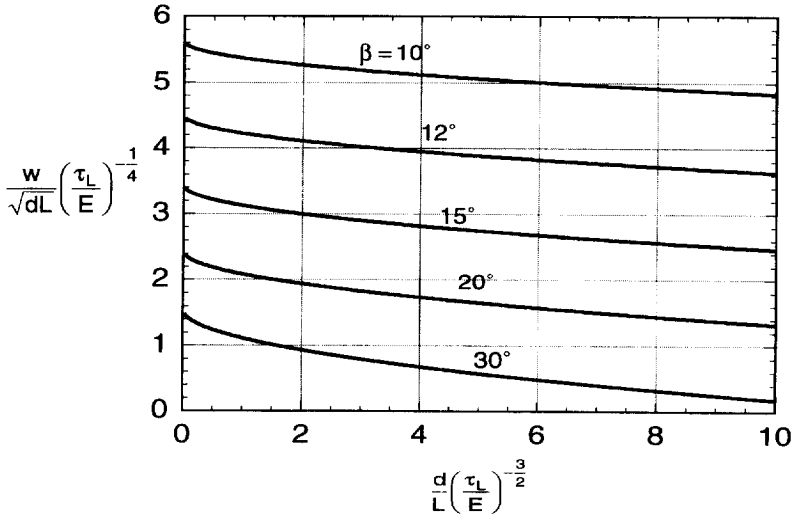

Fig. 8. Length w of downstream locked kink segment.

A few remarks follow about these calculations and results, before we discuss their significance, or lack thereof, vis-a-vis design.

(a) An asymptotic approximation to (41) for small β gives

$$\frac{\sigma_U}{\tau_L} \approx \frac{\sigma_b}{\tau_L} + \left(\frac{\pi B}{2}\right)^{1/2} \beta^{3/4} \tag{42}$$

where

$$B \equiv \frac{d}{L}\left(\frac{\tau_L}{E}\right)^{-3/2}. \tag{43}$$

Remarkably, if we retain the exact result (24) for σ_b in (42), the difference from the exact answers (41) plotted in Fig. 7 stays well under 1% throughout the range shown.

(b) The small-β results for Δ, W_m and W_τ are

$$\frac{\Delta_{bend}}{d}\sqrt{\frac{\tau_L}{E}} \approx \frac{3\pi\beta^{5/2}}{8}, \quad \frac{4W_m\sqrt{\tau_L/E}}{\tau_L d} \approx \frac{\pi\beta^{3/2}}{2}, \quad \text{and} \quad \frac{4W_\tau\sqrt{\tau_L/E}}{\tau_L d} \approx 2\pi\beta^{3/2} \tag{44}$$

In this approximation the bending strain energy is one-fourth the work of shear stress in the curved part of the kink; the exact ratio W_m/W_τ given by eqns (39)–(40) is only slightly less than 1/4 at $\beta = 30°$. It can be verified that eqns (36) and (44) are consistent with (42).

(c) The calculation of σ_U on the basis of eqns (34)–(35) is entirely equivalent to that implied by the Maxwell stress-displacement diagram shown schematically in Fig. 9. The dots denote the upstream and downstream states of the propagating kink, each at the same shortening Δ, consistent with eqn (34). Equality of the shaded regions ensures that the work done per unit width downstream is the same as that upstream, as specified by eqn (35).

(d) Locked kink widths predicted in Fig. 8 for steady-state transverse propagation

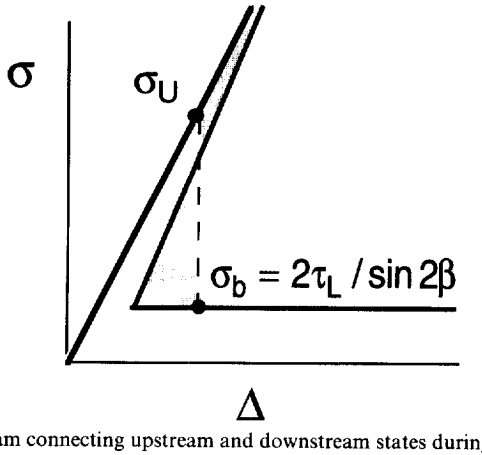

Fig. 9. Maxwell diagram connecting upstream and downstream states during kink propagation.

can be much greater than the sizes of kink segments bounded by fiber breaks and studied by Fleck *et al.* (1995). For example, $\tau_L/E = 0.0008$, $\beta = 15°$, and $d/L = 10^{-4}$ give $w/d \approx 48$; from Fleck *et al.* (1995), we find that for $\tau_Y/E = 0.0004$ and a fiber failure strain equal to 0.015, the broken-segment size is $w/d \approx 16$.

(e) If kinking does not occur until a shortening Δ larger than the critical value $\sigma_U L/E$ for steady propagation has been imposed, we can expect accelerating transverse kink propagation under this fixed Δ. When the process is completed, the stress will have dropped to σ_b, and a locked-up, broadened kink can be expected to extend transversely across the full width of the specimen. The size of the locked portion of the kink could then be estimated by

$$w = \frac{\bar{\Delta} - \sigma_b L/E - \Delta_{bend}}{1 - \cos 2\beta} \approx \frac{\bar{\Delta} - \sigma_b L/E - (3\pi\, d/8)\beta^{5/2}(\tau_L/E)^{-1/2}}{1 - \cos 2\beta}. \tag{45}$$

(f) We have so far ignored the possible effects of testing-machine compliance in the analysis of transverse propagation. This extra compliance can be roughly taken into account by replacing the specimen length L, wherever it appears in any of the results, by a larger effective length L'.

DISCUSSION AND CONCLUDING REMARKS

It will not have escaped the reader's attention that we have taken the kink angle β as a prescribed quantity in our treatments of both band broadening and transverse propagation, but have said nothing about how β is to be chosen. The β question has come up repeatedly in the literature, and suggestions of varying degrees of plausibility have been offered to predict kink angles. A wide variety of β's have actually been observed, and simple theoretical criteria for β based only on analyses of final, uniform kinked states are not promising. Sutcliffe and Fleck (1997) have made extensive numerical 2-D finite element studies of kink initiation, evolution, and propagation, showing clearly how kink fronts reorient themselves naturally as they propagate in order to point in stabilized β directions. But while the dependence of β on various physical parameters was studied, and trends discerned, easy recipes are not yet available. So in the present work, we leave β unspecified.

But this may not matter much when we consider what roles the band-broadening stress or the transverse propagation stress might play in design. Because both are deterministic quantities, not sensitive to initial imperfections, waviness, or notches, it is enticing to adopt one or the other as a design limit, but a glance at their magnitudes is sobering. Assuming $\beta < 20°$, we could say (Fig. 7) that kink propagation could not occur if we kept $\sigma/\tau_L < 3$. But this would constitute a severe restriction. For example, take $\tau_L = 2\tau_Y$ and $\gamma_Y = 0.01$; then, the propagation stress $\sigma = 6\tau_Y$ is substantially less than the peak kinking stresses $\sigma_c \approx 16\tau_Y$ given by eqn (3) for an imperfection $\bar{\phi} = 3°$. This is just an example, but it highlights the dilemma facing the composites designer: he or she must come to grips with the statistics and control of imperfections, echoing the similar situation long faced by engineers who design shells against buckling. Picking σ_U, or the even lower band-broadening stress σ_b, as the design stress is unduly

conservative. On the other hand, the availability of continued deformation at the band-broadening stress confers a welcome pseudo-ductility on the composite after its initial kinking stress is reached.

Finally, we suggest that the present results found for the band-broadening stress, derived on the assumption that there is no fiber fracture, remain approximately applicable when multiple fiber fracture occurs (Fig. 3). During band broadening under increasing shortening, the applied stress can be expected to oscillate if fibers break and lock-up proceeds in discrete steps, not necessarily in unison all along the kink band; but the average stress during broadening should be about the same as that for intact fibers.

ACKOWLEDGEMENTS

This work was supported by NSF (award 92161350), DARPA (subagreement KK3007 with the University of California at Santa Barbara), ONR (contract 0014-91-J-1916), the Division of Engineering and Applied Sciences, Harvard University, and the Department of Engineering, Cambridge University.

REFERENCES

Argon, A. S. (1972) Fracture of composites. *Treatise of Materials Science and Technology*, Vol. 1. Academic Press, New York.

Budiansky, B. and Fleck, N. A. (1993) Compressive failure of fibre composites. *Journal of the Mechanics and Physics of Solids* **41**(1) 183–211.

Budiansky, B. and Fleck, N. A. (1994) Compressive kinking of fiber composites: a topical review. *Applied Mechanics Review* **47**(6), part 2.

Fleck, N. A. (1997) Compressive failure of fibre composites. *Advances in Applied Mechanics*. Academic Press, New York, **33**, 43–117.

Fleck, N. A. and Budiansky, B. (1991) Compressive failure of fibre composites due to micro-buckling. *Proceedings of the 3rd Symposium on Inelastic Deformation of Composite Materials*. Troy, New York, 29 May–1 June 1990, ed. G. Dvorak, pp. 235–273. Springer Verlag, New York.

Fleck, N. A. and Jelf, P. M. (1995) Deformation and failure of a carbon fibre composite under combined shear and transverse loading. *Acta Metall. et Mater.* **43**(8), 3001–3007.

Fleck, N. A. and Shu, J. Y. (1995) Microbuckle initiation in fibre composites: a finite element study. *Journal of the Mechanics and Physics of Solids* **43**(12), 1887–1918.

Fleck, N. A., Deng, L. and Budiansky, B. (1995) Prediction of kink width in fiber composites. *Journal of Applied Mechanics*, **62**, 329–337.

Fleck, N. A., Sivashanker, S. and Sutcliffe, M. P. F. (1997) Compressive failure of composites due to microbuckle growth. *Eur. J. Mech. A/Solids* **16**, 65–82.

Kyriakides, S. and Ruff (1997) Aspects of the failure and postfailure of fiber composites in compression. *Journal of Composite Materials* **31**(20), 2000–2037.

Kyriakides, S., Arseculeratne, R., Perry, E. J. and Liechti, K. M. (1995) On the compressive failure of fiber reinforced composite. *International Journal of Solids and Structures* **32**(6/7), 689–738.

Liu, X. H. and Shih, C. F. (1996) Micromechanics of compressive kinking in composites. *Acta Mater.*, submitted.

Liu, X. H., Moran, P. M. and Shih, C. F. (1996) The mechanics of compressive kinking in

unidirectional fiber reinforced ductile matrix composites. *Composites Part B (Engineering)*, **27B**(6), 553–60.

Moran, P. M. and Shih, C. F. (1998) Kink band propagation and broadening in ductile matrix fiber composites: experiments and analysis. *International Journal of Solids and Structures* **35**(15), 1709–1722.

Moran, P. M., Liu, X. H. and Shih, C. F. (1995) Kink band formation and band broadening in fiber composites under compressive loading. *Acta Metall. et Mater.* **43**(8), 2943–2958.

Rosen, B. W. (1965) Mechanics of composite strengthening. In *Fibre Composite Materials, Am. Soc. Metals Seminar*, Chap. 3.

Schultheisz, C. R. and Waas, A. M. (1996) Compressive failure of composites, Part I: testing and micromechanical theories. *Prog. Aerospace Sci.* **32,** 1–42.

Sivashanker, S., Fleck, N. A. and Sutcliffe, M. P. F. (1996) Microbuckle propagation in a unidirectional carbon fibre–epoxy matrix composite. *Acta Mater.* **44**(7), 2581–2590.

Sutcliffe, M. P. F. and Fleck, N. A. (1994) Microbuckle propagation in carbon fibre–epoxy composites. *Acta Metall. et Mater.* **42**(7), 2219–2231.

Sutcliffe, M. P. F. and Fleck, N. A. (1997) Microbuckle propagation in fibre composites. *Acta Mater.* **45**(3), 921–932.

Vogler, T. J. and Kyriakides, S. (1997) Initiation and axial propagation of kink bands in fiber composites. *Acta Mater.* **45,** 2443–2454.

Waas, A. M. and Schultheisz, C. R. (1996) Compressive failure of composites, Part II: experimental studies. *Prog. Aerospace Sci.* **32,** 43–78.